Chitosan: poly(vinyl) alcohol composite alkaline membrane incorporating organic ionomers and layered silicate materials into a PEM electrochemical reactor

Leticia García-Cruz, Clara Casado-Coterillo, Jesús Iniesta, Vicente Montiel, Ángel Irabien

Journal of Membrane Science

VOLUME: 498, 395-407, 2016

Page:395-407

2016

http://dx.doi.org/10.1016/j.memsci.2015.08.040

Chitosan:poly (vinyl) alcohol composite alkaline membrane incorporating organic ionomers and layered silicate materials into a PEM electrochemical reactor

Leticia García-Cruz[1], *Clara Casado-Coterillo*[2,*], *Jesús Iniesta*[1], *Vicente Montiel*[1], *Ángel Irabien*[2]

[1] Department of Physical Chemistry and Institute of Electrochemistry, Universidad de Alicante, 03080 Alicante, Spain.

[2] Department of Chemical and Biomolecular Engineering, Universidad de Cantabria, 39005 Santander, Spain.

*Corresponding author: Clara Casado Coterillo clara.casado@unican.es

Abstract

Mixed matrix membranes (MMM) are prepared from equivalent blends of poly (vinyl alcohol) (PVA) and chitosan (CS) polymers doped with organic ionomers 4VP and AS4, or inorganic layered titanosilicate AM-4 and stannosilicate UZAR-S3, by solution casting to improve the mechanical and thermal properties, hydroxide conductivity and alcohol barrier effect to reduce the crossover. The structural properties, thermal stability, hydrolytic stability, transport and ionic properties of the prepared composite membranes were investigated by scanning electron microscopy (SEM), X-ray diffraction (XRD), thermo-gravimetric analysis (TGA), water uptake, water content, alcohol permeability, thickness, ion exchange capacity (IEC) and OH^- conductivity measurements. The addition of both organic and inorganic fillers in a CS:PVA blend polymer enhances the thermal and ionic properties. All the membranes are homogenous, as revealed by the SEM and XRD studies, except when stannosilicate UZAR-S3 is used as filler, which leads to a dual layer structure, a top layer of UZAR-S3 lamellar particles bound together by the polymer matrix and a bottom layer composed mostly of polymer blend. The loss of crystallinity was especially remarkable in 4VP/CS:PVA membrane. Thus, the 4VP/CS:PVA membrane exhibits the best ionic conductivity, whereas the UZAR-S3/CS:PVA membrane the best reduced alcohol crossover. Finally, the performance of the CS:PVA-based membranes were tested in a Polymer Electrolyte Membrane Electrochemical Reactor. (PEMER) for the feasibility use of alkaline anionic exchange membranes in electrosynthesis under alkaline conditions, showing the 4VP/CS:PVA and UZAR-S3/CS:PVA membranes the best performances in PEMER.

Keywords: alkaline anion exchange membrane (AAEM); mixed matrix membrane; organic ionomers; layered silicates AM-4 and UZAR-S3; PEMER.

Introduction

The development of fuel cells has allowed the introduction of membranes into the field of electrochemical synthesis of organic products. In this regard, our research group has developed a new concept of Polymer Electrolyte Membrane Electrochemical Reactor (PEMER) based on a polymer electrolyte membrane (PEM) fuel cell for the electro-reduction of model compounds, e.g., cysteine and hydrogenation of acetophenone [1, 2] under acidic conditions, in which the supporting electrolyte consists of a cationic exchange membrane. The PEMER configuration can be also used under alkaline conditions for electro-oxidative processes of alcohols to its carboxylic acids, where the alkaline anionic exchange membrane (AAEM) is a fundamental part for the reaction performance. Most of research studies are mainly focused on fuel cells for direct alcohol oxidation where the AAEM is the main component [3, 4]. Alkaline conditions gets advantages to overcomes the problems found in fuel cells or similar electrochemical devices, e.g., PEMER reactor, using Nafion proton exchange membranes [5]. Several of the reasons are listed below:

- AAEM in alkaline media are the best alternative to Nafion membranes for the use in fuel cells or similar electrochemical devices and configurations since AAEM are less expensive than proton exchange membranes. Furthermore, the use of AAEM in alkaline conditions takes advantage from the use of non precious metal as catalysts, non carbonate formation, crossover reduction and fast electrode kinetic of oxygen reduction reaction.
- Some electrosynthetic processes are more favourable in alkaline media rather than acidic media [6].

- Alkaline media are generally less corrosive, which decreases the cost of the metal electrodes necessary in electrochemical devices [6, 7].

Despite advances reached in the manufacturing of commercial AAEM for a wide number of applications, e.g. desalination, electro dialysis for demineralisation and acid recovery and, more specifically fuel cells, there are still some limitations regarding physical and mechanical properties and durability to be used in fuel cells. Sometimes, the rigid structure of anionic commercial membranes makes difficult the contact between the components of PEM configuration, which is reflected in the performance of electrochemical devices. An AAEM can be competitive and an excellent option in fuel cells or similar configurations when its properties comprise low alcohol permeability [6, 7], high ion exchange capacity (IEC) and consequently low resistance to the transport of hydroxyl (OH^-) ions through-plane (ionic conductivities over 0.1 mS cm^{-1}) [4].

In this regard, a promising alternative to synthetic petroleum-derived polymers and commercial membranes is the chitosan (CS) polymer from natural resources [8, 9]. CS is a low cost and eco-friendly weak polycation with exchangeable NH_2 functional groups that can contribute to the ionic conductivity when the polymer is swollen and OH^- groups that can act as electron donors in addition to amino groups [4]. This led to the introduction of this polymer in recent reviews of fuel and biofuel cells both as polymer electrolyte and as binder and ionic conductor, and also in the electro-catalysts preparation of the electrodes [4, 8]. CS presents a high degree of hydrophilicity which allows the study of this polymer in high temperature conditions, pervaporation separations (separation of various solvents, gaseous mixtures and bio macromolecules) [10-12] and biomedical area (anti- bacterial coatings for medical devices and biocompatible coatings of biomaterials, among others) [13, 14]. The alcohol permeability is low and its use in

alkaline fuel cells has been reported as potentially be able to decrease the carbonation problem affecting the membrane durability [4]. Moreover, CS membranes present a semi-crystalline, less rigid, structure leading to more close contact between catalyst layers or electrodes and membrane, presumably facilitating the OH^- pass from side to side, which probably improves the electrochemical performance. Nevertheless, ionic conductivities are still far from those values recommended for technical applications. For this reason, CS polymer is commonly doped or modified either with inorganic and organic salts or blended with other polymer or polymer mixtures in order to generate ion exchange sites and thereby significantly enhancing the ionic conductivity of the mixed matrix membranes (MMM), as well as increasing mechanical, hydrolytic and thermal stability [4]. Previous works have reported the influence of inorganic fillers on the proton conductivity and performance in direct alcohol fuel cells such as organophosphorilated titania submicrostructure [15], nanosized solid super acid inorganic fillers [16] and zeolites [17]. Recently, we have prepared novel layered titano-and stanno-silicates, ionic liquids and tin particles into a CS pristine membrane matrix [18].

Polyvinyl alcohol (PVA) polymer has been found in the literature as a potential blend polymer of CS for the amelioration of the mechanical, chemical and electrochemical properties of CS ion-exchange membranes [19, 20]. PVA shows a high hydrophilicity, large water permeation and low alcohol crossover [21], essential properties for applications in direct alcohol fuel cells. Moreover, hydroxyl groups from PVA form strong hydrogen bonding with amino and hydroxyl groups of CS enhancing conductivity and mechanical properties [22]. In addition, both polymers are miscible in one another. However, even though the CS:PVA composite anionic exchange membrane doped with KOH enhances the stability and the ionic conductivity of the pure polymer membrane [23], the incorporation of different fillers of inorganic nature can also be used

in this MMM to improve the mechanical, thermal and chemical properties, without decreasing the ion exchange capacity or ion conductivity. In this regard, CS:PVA composite membranes have been modified recently by the incorporation of reduced graphene oxide exhibiting a superior increase in tensile strength and glass transition temperature than those presented by pristine CS:PVA [24] and enhancement of the ionic conductivity and reduction of alcohol permeability [25] was observed when using graphene or sulfonated graphene. As far as the use of organic fillers is concerned, Zhang *et al.* performed the preparation of proton-conducting composite membranes, comprising of Nafion® ionomer into a composite membrane based on CS:PVA blends increasing the proton conductivity and decreasing the methanol permeability of CS:PVA membranes [26].

To the best of our knowledge, the use of anionic resins (anionic ionomers) into the CS:PVA polymer matrix is not yet explored. In this regard, the incorporation of anionic ionomers into the membrane matrix can facilitate the OH^- transport through the membrane since the anionic resin involves a cationic group that will be incorporated as exchange group. Ogumi [27] employed the ion exchange cross-linked, methyl chloride quaternary poly(4-vinylpyridine) resin salt (Figure 1A) binder as electrolyte in the electrode layers, but not yet as a filler in a CS:PVA MMM in order to reduce the alcohol permeation and enhance the electrochemical performance. Moreover, the organic ionomer AS4 has been also used in commercial membrane manufacturing, offering good performance in alkaline direct alcohol fuel cells, although no conclusive feedback can be withdrawn since the physicochemical characteristics of the AS4 ionomer belong to Tokuyama Corp. [28].

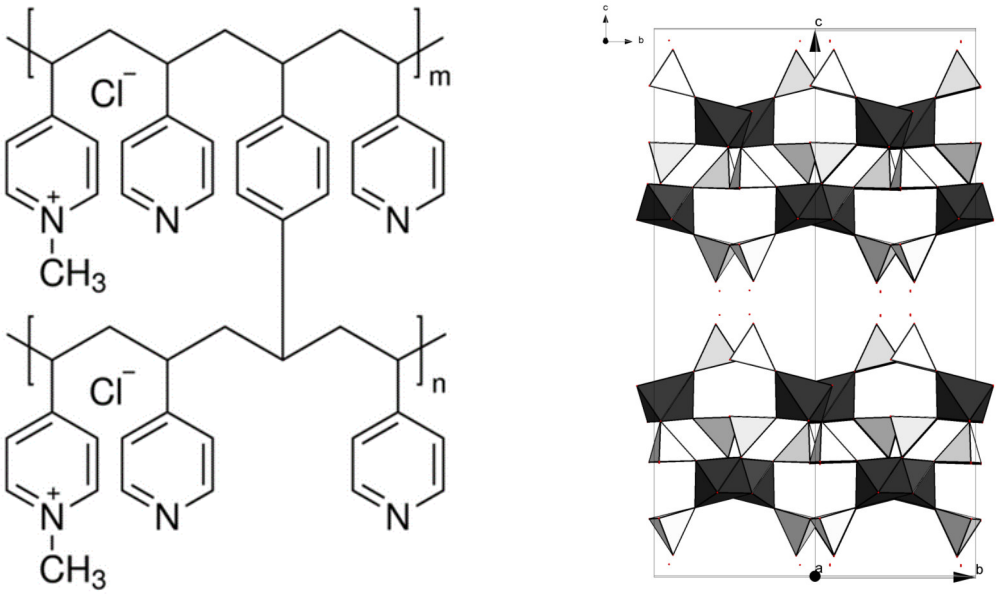

(a) **(b)**

Figure 1. Structure of laminar inorganic and organic fillers: (a) Poly(4-vinylpyridine) cross-linked, methyl chloride quaternary (4-VP), and (b) (0 0 1) projection of AM-4 titanosilicate.

Our objective is to improve the performance of electrosynthesis reactions in high alkaline media by the synthesis of membranes with improved physical, mechanical properties and ionic conductivity that let us expect a better electrochemical performance in alcohol electrooxidation. In this work, we have synthesised CS:PVA MMM, doped with layered UZAR-S3 stannosilicate [9], AM-4 titanosilicate [10], whose structure is drawn in Figure 1B, as inorganic fillers, anionic poly (4-vinylpyridine) (4VP) ionomer, in Figure 1A [29], a cross-linked, methyl chloride quaternary salt, whose molecular structure is drawn in Figure 1A, or AS4 ionomer [30, 31], whose molecular structure has not been disclosed by the company, respectively. The MMM synthesised have been characterised by SEM, XPS, XRD and TGA techniques. Water uptake, alcohol permeability and ion-exchange capacity were also measured as a function of membrane composition. The ionic conductivity was obtained by electrochemical impedance

spectroscopy. The MMM behaviour upon the electrooxidation of water and propargyl alcohol in alkaline conditions have been conducted through polarisation curves using a PEMER configuration.

Experimental section

2.1 Materials and chemicals

Chitosan (CS, coarse ground flakes and powder, Sigma-Aldrich, Spain) with a molecular weight from 310,000 to > 375,000 and 75 % deacetylation degree, based on the viscosity range 800-2,000 mPa s, and Poly(vinyl) alcohol (PVA, 99+% hydrolysed from Sigma Aldrich, Spain) with a molecular weight 85,000-124,000 were used as purchased. Reactants for the synthesis of layered titanosilicate AM-4 and UZAR-S3 were used as purchased. The ion exchanged poly (4-vinylpyridine) cross-linked, methyl chloride quaternary salt resin (4VP) that was used as ionomer filler as purchased from Sigma Aldrich. AS4 ionomer filler was used as purchased from Tokuyama Company, Japan. All other chemicals were purchased from the highest analytical grade available and were used as received without any further purification. Doubly distilled water with a resistivity of 18.2 MΩ cm was used for all solutions preparation.

Lamellar microporous titanosilicate AM-4 was synthesised by a seeded secondary-growth procedure reported in a previous work [32]. A typical seeded synthesis (to produce about 2.5 g of solid) was as follows: NaOH pellets, distilled water, and TiO_2 (99.8 wt. %, Sigma Aldrich) were added to a Na_2SiO_3 solution (27 wt. % SiO_2, 8 wt. % Na_2O, Merck). A gel with molar composition 4.2 SiO_2:TiO_2:2.9 Na_2O:68 H_2O and a pH of 12.1, was formed and stirred at room temperature for 1 h and seeded with AM-4, previously prepared. Then, this gel was introduced into a Teflon-lined autoclave and heated in an oven at 230 °C for 24 h. The autoclave was then quenched in tap water and the white solid filtered and washed repeatedly and dried at 100ºC overnight. AM-4 is

composed of Ti and Si pyramid layers separated by galleries containing Na^+ ions accounting for their high ion-exchange capacity [33].

Layered microporous UZAR-S3 ($Na_7Sn_2Si_9O_{25}$) was synthesised by a similar procedure [34]. In a typical synthesis to produce 4 g of solid, 19.1 g gel were prepared from the sodium silicate solution (27 wt.% SiO_2, 8 wt.% Na_2O, Merck) mixed with deionized water and NaOH (98 wt.%, Sigma Aldrich). Tin (II) chloride dehydrate (reagent grade 98 wt. %, Sigma Aldrich) was then added. After stirring for 1.5 h at room temperature, the resulting gel was degassed for a few minutes in an ultrasonic bath and transferred to a 40 mL Teflon-lined autoclave. The crystallization was carried out under hydrothermal conditions at 230 ºC for 96 h, before filtering and washing repeatedly with deionised water, and dried at 100 ºC overnight.

2.2 Membrane preparation

CS:PVA blend membranes and MMM were prepared from a mixture of 1 wt. % CS and 4 wt. % PVA solutions according to previously reported procedures with slight modifications [35]. Briefly, CS powder was added to the acetic acid/water mixture and stirred at room temperature for 24 h. In a separate beaker, PVA powder was added to distilled water until saturation and was refluxed at 85 ºC for 2 h. Then, CS and PVA solutions were filtrated. Finally, the blend membrane was prepared to CS:PVA ratio of 50:50 wt. % by mixing the appropriate amounts of the single polymer solutions and stirring till a homogeneous mixture was observed. Then, the CS:PVA solution was degassed in the ultrasound bath and cast on a glass plate using a doctor blade knife at a 0.15 mm opening. The solvents were evaporated at room temperature in a fume-hood for 2 days. The ion exchange was carried out by immersion in 1.0 M NaOH bath for 24 h and

then thoroughly washed with distilled washing to remove the NaOH excess. Finally, the membranes were ready for further characterization. The membranes were noted as Filler Name/CS:PVA, where the fillers are AS4, 4VP, AM-4 or UZAR-S3, and the content of the filler is 5 wt. % to the total polymer matrix unless otherwise stated.

MMM were prepared by adding the distinct fillers (4VP and AS4 ionomers, AM-4 and UZAR-S3 layered silicates) to the homogeneous CS:PVA blend solution, before the degassing in ultrasound bath, and the mixture was hence stirred for 24 h until homogeneity. The AM-4 and UZAR-S3 layered silicates fillers were dispersed in a few milliters of ultrapure water previously to the addition to the polymer solution. In all cases studied in this work, the filler composition was 5 wt. % with respect to total polymer, since previous essays at higher concentrations (20 wt. %) led to difficult dispersion and decreased membrane [18]. The different filler-polymer mixtures were degassed in the ultrasound bath and cast on a glass plate using a doctor blade knife at the same opening as the CS:PVA blend membranes. Likewise, MMM were immersed into 1.0 M NaOH renewable solution for 24 h in order to carry out the ion exchange. In all cases, membranes were ion exchanged for different times from several hours to a few days to study the effect of additives on chemical stability.

The membrane thickness was measured with an IP-65 digital micrometre with a precision of 0.001 mm (Mitutoyo Corp., Japan), at least 4-5 spots over the membrane surface. The weight of the dry membranes was also measured at this point in an electronic balance with a precision of 0.001 g.

2.3 Physicochemical characterisation

The morphology of the CS:PVA membranes was observed by scanning electron microscopy (SEM) and was performed on both the surface and cross-section of the

samples using a Zeiss DMS 942 instrument operating at 30 kV. Cross-section images for all membranes were obtained according to the following procedure: the membranes in OH^- form were dried at room temperature in a Petri dish; next, the membranes were immersed in liquid nitrogen for few seconds and finally, they were cut in order to get a representative cross section image of the membrane.

X-ray photoelectron spectroscopy (XPS) experiments were recorded on a K-Alpha Thermo Scientific spectrometer using AlKα (1486.6 eV) radiation, monochromatised by a twin crystal monochromator and yielding a focused X-ray spot with a diameter of 400 μm, at 3 mA × 12 kV. Deconvolution of the XPS spectra was carried out using a Shirley background.

The X-ray diffraction patterns of the membranes were collected on a Philips X Pert PRO MPD diffractometer operating at 45 kV and 40 mA, equipped with a germanium Johansson monochromator that provides Cu Kα1 radiation (λ = 1.5406 Å), and a PIXcel solid angle detector, at a step of 0.05º. The crystallinity of the membranes was examined at 25 ºC by powder X-ray diffraction Bruker D8-Advance with mirror Goebel (non-planar samples) with a generator of X-ray KRISTALLOFLEX K 760-80F (power: 3000 W, voltage: 20-60 kV and current: 5-80 mA) with a tube of X-rays in the wave length 1.5406 – 1.54439 Å.

Thermal gravimetric analyses (TGA) were carried out using a DTG 60H Shimadzu instrument (Japan) under nitrogen from 25 to 700 °C at a heating rate of 10 °C min^{-1}, in order to study the thermal stability of the resulting membrane materials. The decomposition temperature was calculated as the temperature at which 5 % weight loss occurs, once the excess water has been removed from the sample.

The water uptake (W_u) or swelling of CS:PVA-based membranes was calculated by measuring the change in weight of the membrane before and after hydration, *i.e.,* the

process of adsorption of large quantities of water molecules by the membrane, which resulted on a swelled membrane with a considerable increase in volume. The OH^- form of the membrane was immersed in deionized water at room temperature and equilibrated for 24 h. By removing the excess water and weighing the membrane in a precision balance the wet weight of the membrane, W_{wet}, was determined. The percentage of water uptake was thus calculated using equation (1)

$$W_U \; or \; swelling\,(\%) = \frac{W_{wet} - W_{dry}}{W_{dry}} \times 100 \qquad (1)$$

where W_{dry} is the weight of the dried membrane.

Likewise, since the CS-based membranes are so hydrophilic that any interpretation of these parameters may be confusing, the bound water content was also measured from the TGA curves, according to Franck-Lacaze *et al.* [36] using equation (2). The water content, WC, was estimated from sample masses m_1 and m_2, measured at T_1 and T_2, taken at the minimum observed between the two peaks of the differential spectrum (one for water vaporization, one for polymer degradation), respectively.

$$WC\,(\%) = 100\left(1 - \frac{m_2}{m_1}\right) \qquad (2)$$

The ion exchange capacity (IEC) is commonly measured by titration. In our work, the dried and weighed membrane was soaked in 1.0 M NaOH renewable solution for 24 h at room temperature. The membrane was thus converted to OH^- form. Then the membrane was rinsed thoroughly with doubly distilled water and equilibrated for 24 h in order to remove the last traces of alkali. In the last step, the membrane was immersed in 0.1 M HCl solution for 24 h and this solution was then titrated by a standardized 0.1 M NaOH solution. The IEC was calculated by equation (3)

$$IEC\left(mmol/g\right)=\frac{\left(V_{NaOH,i}-V_{NaOH,f}\right)\times C_{NaOH}}{W_{dry}}\times 100 \quad (3)$$

where $V_{NaOH,i}$ and $V_{NaOH,f}$ are the volume of 0.1 M NaOH solution consumed during back-titration of HCl solutions without and with membrane and C_{NaOH} is the concentration of NaOH solution previously standardized by hydrogen potassium phthalate [37].

2.4. Electrochemical impedance spectroscopy

The electrochemical impedance spectroscopy (EIS) measurements were carried out in order to obtain the specific conductivity of all membranes synthesised in this work according to described in [38, 39]. EIS experiments were performed using a microAutolab equipped with a FRA impedance module at open circuit potential (potentiostatic method). CS: PVA based MMMs were placed between stainless steel -plated electrodes with a projected geometric area of 1.13 cm^2 and EIS cell was subjected to a constant pressure until the Nyquist plot of the EIS response was repeatedly the same. The amplitude was set at 10 mV and the frequency range was varied between 1 MHz and 100 Hz. The EIS experiments were performed at controlled temperature of 25 ± 3 ºC. Before EIS experiments, membranes were activated in 1.0 M NaOH for 24 h, and then, thoroughly rinsed with ultrapure water and finally stabilised in ultrapure water for 24 h before measurements. The water was removed out the membrane surface using a blotting paper before placing it in the EIS cell. The ionic conductivity σ (mS cm^{-1}) was calculated as usual using equation (4),

$$\sigma=\frac{L}{RA} \quad (4)$$

where L is the distance between both electrodes (cm), A is the surface area of the membrane exposed to the electric field (cm^2) and R is the resistance of the membrane (Ω).

2.5. Alcohol permeability measurements

The alcohol permeability was measured in a home-made diffusion cell at room temperature (20 ºC). The OH^- form membrane previously equilibrated in ultrapure water was sandwiched between the two compartments of a filter-press configuration with 10 cm^2 projected area. The compartments were then clamped among O-Viton joints, with an effective membrane area also of 10 cm^2.The first compartment (A) was filled with a 0.25 M n-propanol in 1.0 M NaOH solution to simulate the reaction medium. The second compartment (B) was filled with ultrapure water. Both compartments were filled up and at the same pressure. The total volume cell was 4-5 mL in each compartment. N-propanol concentration was measured by gas chromatography (GC 2010, Shimadzu, Japan) at the beginning of the experiment and then at different times up to 24 h. However, only at 30 min or 1 h the slope of the curve n-propanol concentration in the B compartment (C_B) vs. time was a straight line. The permeability coefficient of n-propanol, P ($cm^2 \cdot s^{-1}$), was calculated using equation (5),

$$P = \frac{\left(C_B - C_{B0}\right)}{\left(t - t_0\right)} \frac{V_B L}{A C_{A0}} \tag{5}$$

where A (cm^2) and L (cm) are the membrane area and thickness, respectively. C_{A0} (ppm) is the initial concentration of n-propanol in the compartment A, and V_B is the water volume in compartment B.

2.6 Polarisation curves into a PEM electrochemical reactor

The polarisation curves were performed using a home-made Polymer Electrolyte Membrane Electrochemical Reactor PEMER architecture of 25 cm^2 projected area using a current intensity range between 0.02 A and 0.5 A [40]. To obtain a stable potential value,

each established current intensity value was held for 1 min before monitoring the cell potential. The membranes were placed between a Ni supported carbon black electrode (0.1 mg cm^{-2} Ni loading) which acted as anode, and a cathode which comprised a catalytic layer of Pt supported carbon black (0.1 mg cm^{-2} Pt loading) onto diffusion layer (2.0 mg cm^{-2} Vulcan XC-72). 1.0 M NaOH solution was used in order to feed the anodic compartment with a flowrate of 12 mL min^{-1}. Humidified synthetic air (99.999%) was fed into the cathode with a flow rate of 50 mL min^{-1}.

3. Results and discussions

3.1 Physicochemical characterization

Different types of MMMs based on the CS:PVA blend are prepared by varying the type of filler: AS4 and 4VP ionomers, and layered materials such as AM-4 titanosilicate and UZAR-S3 stannosilicate, in 5 wt. % loading regarding the total polymer unless otherwise stated. The membrane thicknesses oscillate between 40 and 100 μm, with a yellowish transparent appearance except those containing UZAR-S3 and 4VP, which turn white and lightly yellow, respectively (as shown in Figure 2). They also seem homogeneous with a good mechanical flexibility and robustness upon manipulation.

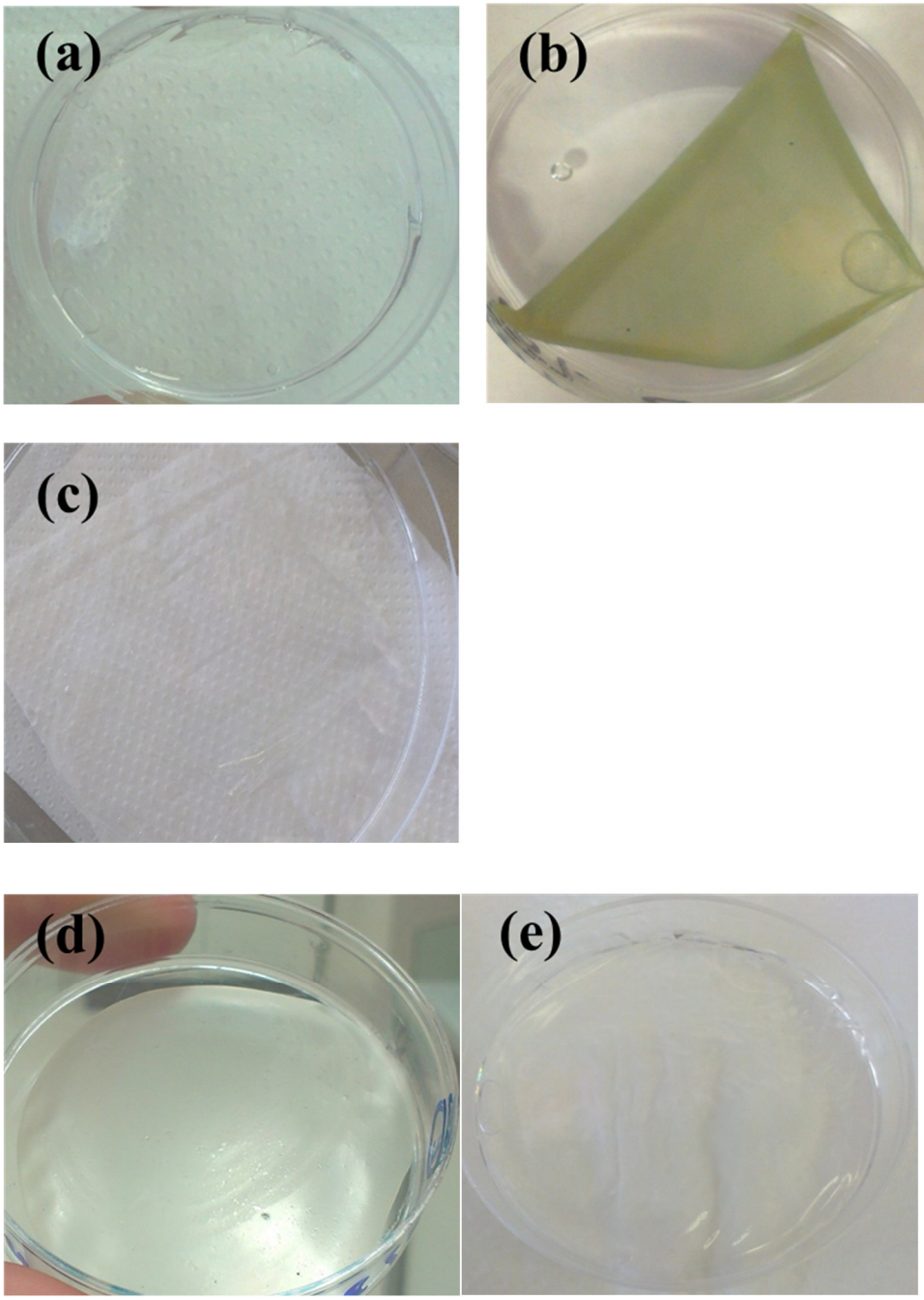

Figure 2. Photography's of the CS:PVA- based membranes synthesised: (a) pristine CS:PVA blend, (b) 4VP/CS:PVA MMM, (c) AS4/CS:PVA MMM, (d) UZAR/S3/CS:PVA MMM and AM-4/CS:PVA MMM.

Figure 3 shows the SEM images of the surface and cross section morphology of the CS:PVA membrane as well as the different MMMs. The incorporation of the AM-4, 4VP and AS4 fillers provide both homogenous dispersion across the bulk of the CS:PVA based membrane and a smooth and flat surface alike, whereas in the case of the UZAR-S3/CS:PVA MMM, the UZAR-S3 stannosilicate is uniformly dispersed only on the membrane. The behaviour of UZAR-S3 additive when blended with polymer matrix is similar to that previously reported by García-Cruz *et al*. [18], where it was observed that these inorganic particles were not incorporated within the CS matrix, but a dual-layer structure is formed, where the inorganic filler UZAR-S3 provides a thin film onto polymer matrix surface. In that case, the pure polymer was filled with 20 wt. % UZAR-S3 with respect to the mass of polymer. In this work, we observe the same behaviour at the low loading of 5 wt. %. Hence, the amount of UZAR-S3 particles has no influence on the dispersion of the filler itself in polymer matrix. This dual-layer structure has been obtained lately in the MMM literature [41, 42] for zeolite A/PTMSP and ZIF-8/PEBA MMM, where the permeation behaviour was assimilated to a pure inorganic membrane that was obtained by the simple MMM preparation method.

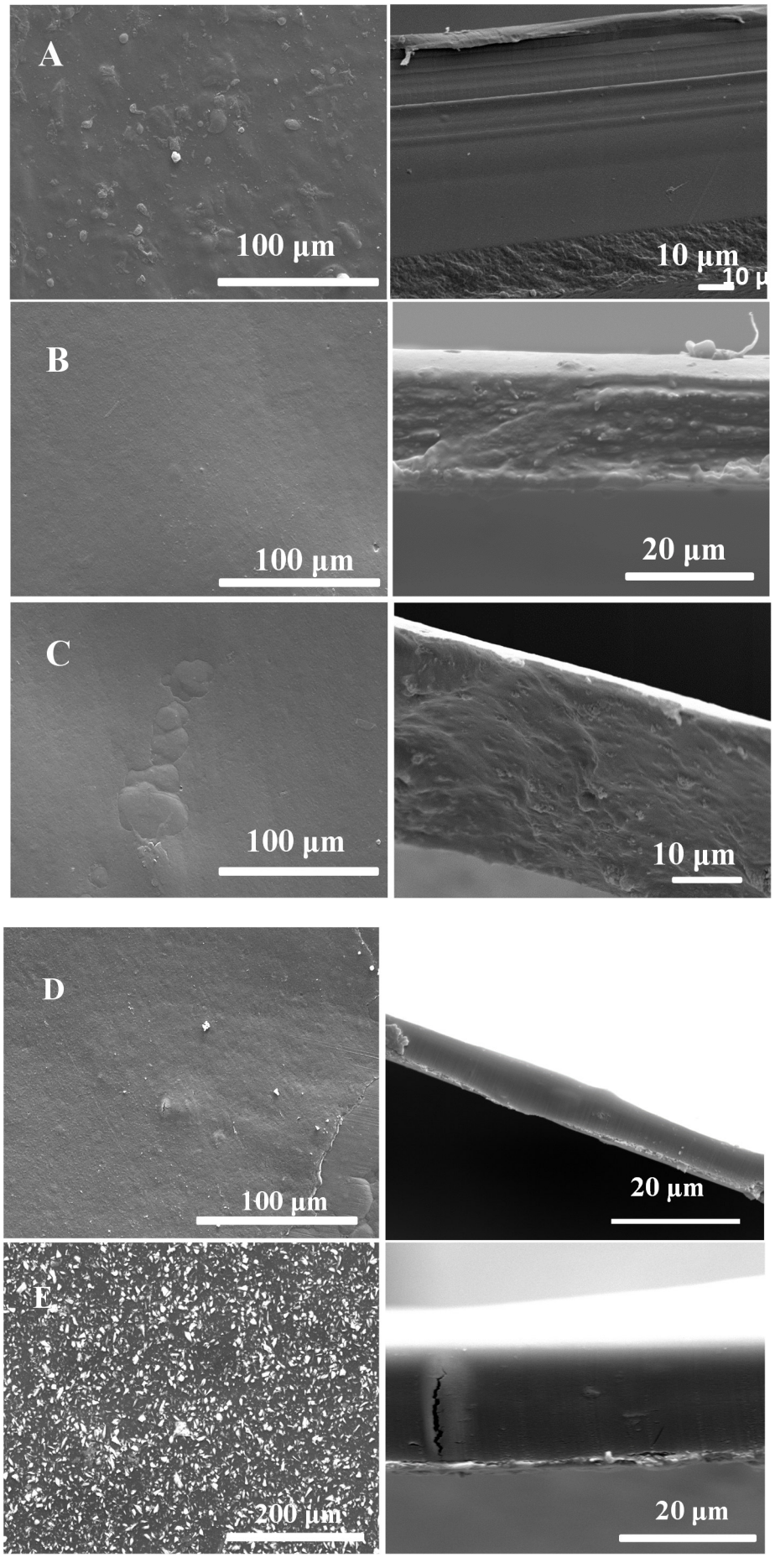
A
100 µm
10 µm
B
100 µm
20 µm
C
100 µm
10 µm
D
100 µm
20 µm
E
200 µm
20 µm

Figure 3. SEM micrographs of the CS:PVA-based membranes: (A) pristine CS:PVA, (B) AS4/CS:PVA, (C) 4VP/CS:PVA, (D) AM-4/CS:PVA, (E) UZAR-S3/CS:PVA. Figures represent the topographical surface (left column) and cross-sectional (right column) view of the membranes.

The cracks observed in some of the images in Figure 3 are due to experimental observation under the electron beam. For instance, a comparison of the cross section of the AM-4/CS:PVA prepared in this work with that of AM-4/CS membrane [18] proved that both membranes presented good dispersion and distribution of the AM-4 particles, regardless of the CS ratio in the polymer blend. Both membranes showed no cracks or fractures throughout the membrane thickness. The addition of the AM-4 and UZAR-S3 inorganic fillers, as the organic AS4 and 4VP ionomers mixed homogeneously with the CS:PVA blend membrane.

In fact, all membranes synthesised in this study were subjected to polarisation experiments by using a PEMER electrochemical filter press reactor. Mechanical stability of all CS:PVA based membranes was proved by successive assembly and disassembly of the electrochemical reactor, where all membranes revealed no cracks or fractures. Besides, the SEM images of membranes after using in a reactor PEMER again proved neither morphological changes in plane cross section in all membranes tested nor presence of cracks or fractures (not shown).

Table 1. Deconvolution of the XPS Spectra obtained for the CS:PVA, AS4/CS:PVA, 4VP/CS:PVA, UZAR-S3/CS:PVA, and AM-4/CS:PVA MMMs, and the assignments based on the binding energy.

Element	CS:PVA	AS4/CS: PVA	4VP/CS:PVA	UZAR-S3/ CS:PVA	AM-4/CS: PVA
C 1s	284.29 (40.71) C-C-CH	284.27 (62.39) C-C-CH	284.04 (58.15) C-H (283.93), C-C-CH	284.28 (33.1) C-C-CH	284.16 (23.89) C-C-CH
C 1s	285.85 (25.41) C-N, C-H	285.78 (14.35) C-N, C-H	285.56 (15.60) C sp^2, C sp^3, C-N, C-H	285.84 (29.75) C-N, C-H	285.6 (24.08) C-N, C-H
C 1s	287.62 (7.12) -C=O, or -O-C-O-	288.16 (5.70) -C=O, C=O, C-N	287.25 (5.86) C=O, C-O, C-N	287.47 (5.71) -C=O, -O-C-O-	286.84 (11.61) C=O
C 1s					288.03 (4.94) C=O, C-O-C, O-C=O, carboxyle
C %	**73.24**	**82.44**	**79.61**	**68.56**	**64.52**
N 1s	399.15 (4.01) NH-C, NH_2	399.04 (0.79) C-NH-C, NH_2	398.66 (3.11) C-NH-C, NH_2 or pyridine	399 (2.64) C-NH-C, NH_2	398.85 (4.80) C-NH-C, NH_2
N 1s	400.8 (0.68) C-N	400.14 (0.25) C-N	400.01 (0.40) C-N	400.23 (0.45) C-N	401.12 (0.65) C-N
N %	**4.69**	**1.04**	**3.51**	**3.09**	**5.45**
O 1s	531.03 (5.44) OH-	531.5 (9.12) OH-	531.61 (15.79) OH-, or C=O	532.16 (26.76) -OH (532)	531.91 (26.81) OSi (SiC), OH

Element	CS:PVA	AS4/CS: PVA	4VP/CS:PVA	UZAR-S3/ CS:PVA	AM-4/CS: PVA
O 1s	532.22 (16.62) O-C, C=O	532.89 (6.47) SiO_2, - C=O, C-OH, C-O-C	530.37 (1.96)	534.42 (0.86) -C-O	534.25 (2.82) -C-O
O 1s	------	533.97 C-O		------	
O %	**22.06**	**16.38**	**17.75**	**27.62**	**29.63**
Si $2p^3$	------	------	------	101.39 (0.71) Me_2 SiO, aminosilicate sodalite (101.5), SiO_2	101.44 (0.20) Hydroxy sodalite, (MeSiO)n

XPS is performed on the CS:PVA MMM synthesised, where deconvolution of the XPS spectra is shown in Table 1. According to the XPS data, the 1s binding energy of element C and N for the membranes with different fillers do not reveal significant differences. The UZAR-S3/CS:PVA MMM show the binding energy of C and N elements are closest to the pristine CS:PVA membrane, which effectively indicates that the UZAR-S3 particles are located on the membrane top layer and there is an inferior bottom layer composed mainly of the polymers blend, as observed by SEM. All membranes show two peaks at N 1s (399.9 - 400 eV and ca. 401 eV) corresponding to $–NH_2$ or –NH and C-N– groups of CS, respectively, suggesting that there is no complexation of the N atom by the heteroatoms of the organic and inorganic fillers. The major percentage of N atom corresponds to the membrane doped with inorganic AM-4 titanosilicate (5.65 at. %), likely associated to a larger interaction of the amino groups of the CS:PVA matrix with the AM-4 layered particles. In addition, the XPS data of 4VP/CS:PVA MMM prove the

presence of pyridine by the binding energy at 398.66 eV, which comes from the organic ionomer and thus the C-N is remarkable as well as the total percentage of N atom (3.5 at. %) in this membrane. Also, all spectra denote the –C=O presence, which can be attributed to the rest of the acetyl groups from the CS employed, which is not completely deacetylated or, on the contrary, the –C=O groups can also be due to acetic acid adsorption upon membrane preparation. The total percentage of C atom is larger for the membranes doped with organic ionomers, 82.44 % and 79.61 % for the AS4/CS:PVA and 4VP/CS:PVA MMM, respectively, probably due to the insertion of a new carbonated chain in CS:PVA matrix. The binding energy of O element shows a major difference among the membranes prepared. The total percentage of O is major for the AM-4/CS:PVA and UZAR-S3/CS:PVA MMM with respect to pristine CS:PVA, as a result of the O-Si functionalization groups dispersed in the polymer blend. The XPS spectrum also confirms the presence of Si oxides for the membranes with silicate fillers by a binding energy 101.39-101.44 eV. Si content agrees with the elementary composition of the inorganic fillers [43].

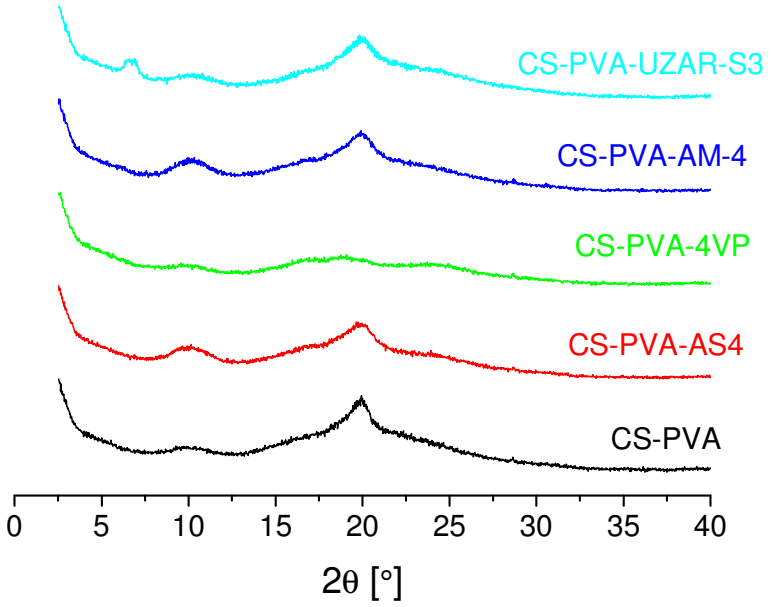

Figure 4. X-ray diffractograms of the CS:PVA-based membranes.

High intensities and sharp peaks in the XRD experiments are related to the crystallinity of the sample. Figure 4 represents the X-ray diffractograms of CS:PVA-based membranes, where we can observe the expected semi-crystalline nature of CS polymer, with broad peaks at 2θ equals to 10º and 20º, corresponding to the crystal forms I and II of CS [12]. The characteristic diffraction band of PVA is located at 2θ = 19.5° [24]. The CS:PVA blend does not reveal changes on the peaks position but the intensity of the peaks is lower than those of pure CS [18] because of the decrease of intermolecular interaction between the polymer blend chains and thus the crystallinity degree is decreased [44]. From the 4VP/CS:PVA diffractograms, it can be observed the disappearance of the characteristics peaks of CS and PVA polymers, meaning that the incorporation of this organic filler leads to the complete destruction of the crystalline character of the polymers. In the XRD diffractograms of AS4/CS:PVA, UZAR-S/CS:PVA, and AM-4/CS:PVA both characteristic peaks are observed at 10º and around

20º corresponding to CS and PVA pure polymers, which indicates that the semi-crystalline character is maintained. In fact, the full width at half maximum (FWHM) obtained for AM-4/CS:PVA (2.8º), AS4CS:PVA (3.15º), UZAR-S3 CS:PVA (3.25º) membranes are higher than that presented by the pristine CS:PVA (1.88º) membrane, which is typical of semi-crystalline polymers. Therefore, the order of crystallinity CS:PVA > AM-4/CS:PVA > AS4/CS:PVA, UZAR-S3/CS:PVA > 4VP/CS:PVA, where there is an inverse relationship between FWHM and the crystallinity of the composite membrane. Therefore, the relative FWHM value for the 4VP/CS:PVA MMM being remarkably higher than those of the others, it can be concluded that the loss of crystallinity of the membrane 4VP/CS:PVA is almost complete. The broadness of the Bragg peaks in the crystalline region is associated to the crystalline nature of the film and the amount of disorder and imperfections. The apparent loss of crystallinity (or increased disorder) observed in the XRD patterns of the AM-4/CS:PVA and UZAR-S3/CS:PVA MMM may be due to the partial exfoliation of the layered precursors into thin lamellar particles. This favours the dispersion of the AM-4 titanosilicate and UZAR-S3 stannosilicate materials in the CS:PVA matrix. This exfoliation is more remarkable in the case of UZAR-S3 by the appearance of a new peak at 6.85º [43], despite the dual-layer structure. The greater amorphousness in AM-4/CS:PVA MMM can thus be attributed to a higher degree of exfoliation [45], probably due to the fact that this layered titanosilicate is dispersed in all the membrane matrix and not only on a top layer.

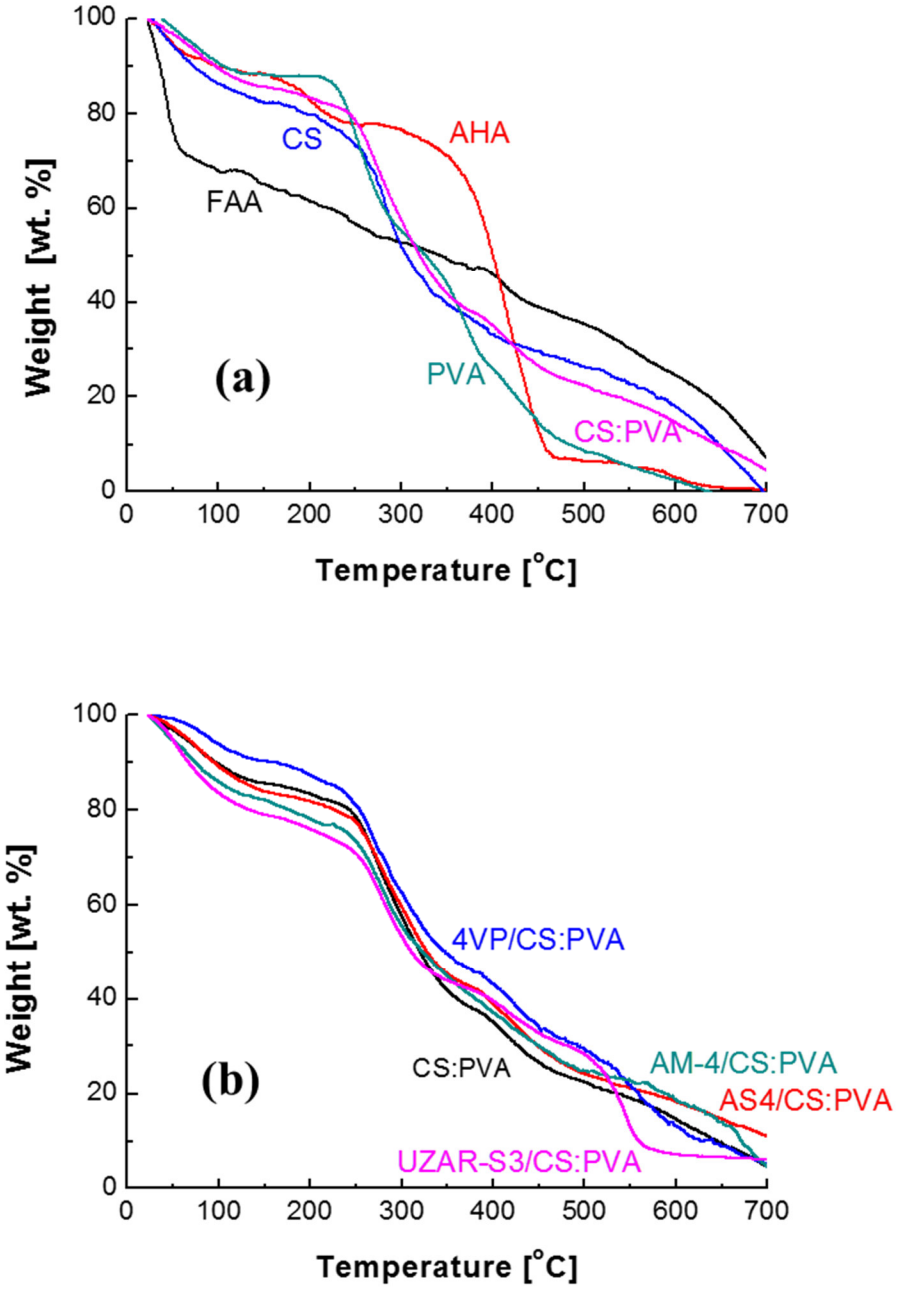

Figure 5. Thermal decomposition of the CS:PVA-based membranes under nitrogen atmosphere: (a) Comparison of pure polymer and commercial membranes and (b) comparison of CS:PVA-based membranes.

The durability of the solid electrolyte membrane is very important for the commercial application in electrochemical devices. Thermal stability apparently plays a

key role since AAEMs have to operate steadily in alkaline environment at different temperatures for long terms [46]. The weight loss of the MMMs is studied under air at a heating rate of 10 ºC min^{-1}. Since the swelling of the polyelectrolyte membranes is one of the factors limiting their performance in fuel cells [47], and the swelling depends on the water adsorption in the membrane, the thermal decomposition of the membranes is verified under nitrogen atmosphere and the TGA curves are represented in Figure 5. The thermal decomposition temperatures and initial weight losses are higher than those reported for other anion-exchange membranes hybridised by silica [48]. Another explanation for this is that the number of thermally stable ammonium and hydroxyl groups available in the membranes is occupied by the adhesion with the inorganic or organic filler groups. Figure 5(a) represents the weight losses occurring in the membrane material upon temperature increase, observing some slight differences in the stages from the homogeneous degradation curve of the pristine PVA membrane [49]. A comparison of TGA experiments of the pure PVA membrane with the CS:PVA blend membrane reveals that the thermal stability is increased around 15 ºC for the later due to the incorporation of CS into the PVA membrane, see also Table 2, and as previously stated by Yan *et al*. [35]. On the other hand, as described in [18, 29], the degradation of CS involves three characteristics stages: a first stage up to 180 ºC, corresponding to the evaporation of the free and bound water in the membrane; a second step up to 450 ºC, corresponding to the elimination of side groups and the beginning of deacetylation and depolymerisation of CS. The third stage begins from 450 ºC for the breakdown of the polymer backbone.

Table 2. Membrane decomposition temperature and weight loss. Data are obtained from TGA curves under nitrogen atmosphere.

Membrane	T_d [ºC]	**Weight loss [wt. %]**
FAA (Fumatech)	140	33.83
AHA (Tokuyama)	310	24.38
CS	260	28.64
PVA	240	18.28
CS:PVA	255	23.11
AS4/CS:PVA	250	22.5
4VP /CS:PVA	260	21.89
AM-4/CS:PVA	250	26.67
UZAR-S3/CS:PVA	255	30.24

The first stage is similar for AS4/CS:PVA and 4VP/CS:PVA and their weight loss is also slightly lower than that shown for the pristine CS:PVA membrane. These differences are attributed to the hydrophobic character imparted by the ionomer, in agreement with literature for polyvinylpyrrolidone-based membranes [36]. The second stage, which is attributed to decomposition or elimination of the side groups of the membrane, occurs between 250-450 ºC for CS:PVA-based membrane [50] and the third stage corresponds to the breakdown of the polymer backbone at temperatures higher than 500 ºC. The onset of the second stage is slightly shifted to higher temperatures when the

CS:PVA blend polymer is filled by 5 wt. % 4VP ionomer. On the contrary, this shifting is not observed when the layered inorganic stannosilicate UZAR-S3 and titanosilicate AM-4 and organic commercial AS4 ionomer are used as filler. However, the thermal stability of CS:PVA-based membranes improve compared to pure PVA membrane. Therefore, the presence of CS and organic or inorganic fillers enhance the thermal stability. From the residual weight of the AM-4 and UZAR-S3/CS:PVA MMM, we can confirm that the inorganic filler loading agrees with the nominal value of 5 wt. %. In summary, the CS:PVA-based membranes have higher thermal stability than the commercial FAA membrane, where the decomposition of membrane begins at 140 ºC (see Table 2 and Figure 5) and the thermal stability is improved by the effect of 4VP addition.

Table 3. Bound water content, water uptake, ion exchange capacity and hydroxide ion conductivity of the membranes prepared in this work.

Membrane	**WC (%) [a]**	**W_U (%)**	**IEC (mmol g^{-1})**	**Conductivity (mS cm^{-1})**
CS	28.64	88.5	0.12	0.07 [18]
PVA	18.28	157.5	0.096 ± 0.018	-----
CS:PVA	23.11	139.5	0.253 ± 0.050	0.15– 0.29
4VP /CS:PVA	21.89	134.0	0.266 ± 0.0 04	1.15
AS4/CS:PVA	22.5	131.5	0.325 ± 0.026	0.32

Membrane	**WC (%)** [a]	**W_U (%)**	**IEC (mmol g^{-1})**	**Conductivity (mS cm^{-1})**
AM4/CS:PVA	26.67	128.3	0.176 ± 0.001	0.38
UZAR-S3/CS:PVA	30.24	121.6	0.310 ± 0.060	0.03
FAA (Fumatech)	33.83	16.19	0.318 ± 0.018	2.92[b]
AHA (Tokuyama)	24.38	21.8	0.352 ± 0.023	3.22[b]

[a] Precision of 3 %. Calculated according to Franck-Lacaze et al. [36] using equation (2).

[b] The conductivity values for commercial membrane were measured in our laboratory at the same conditions of CS: PVA based membrane.

The water content can be calculated from the first stage observed in TGA curves, corresponding to the evaporation of free or bound water. The presence of water in the membrane is usually attributed to a major significance on the ionic conductivity and mechanical strength of anion-exchange membranes. An excessive water content is generally related to a loss of mechanical properties, and an excessive dryness makes the membrane brittle [51]. Table 3 shows the bound water content value of synthesised membranes. There are no significant differences between this water content obtained for each CS:PVA based MMMs in comparison with the commercial membranes. The blend between both polymers decreases from 28.64 % to 23.11 % the water content of pure CS because PVA polymer has hydroxyl groups that bond easily and strongly with water molecules. However, when the organic additives are incorporated in CS:PVA matrix, the water content decrease since their hydrophobic character. The membranes with inorganic

fillers show higher water content because these layered inorganic materials involve hygroscopic groups such as SiO_2, TiO_2 and SnO_2 [12]. This agrees with the thermal analysis above, where a high degree of hydration, and therefore higher water content, is related to a lower degradation temperature with none or slight lower changes for UZAR-S3/CS:PVA and AM-4/CS:PVA- membranes compared to the CS:PVA membrane.

The total water uptake can induce significant swelling, being responsible of the dilution of the anions (OH^-) concentration, which decreases the membrane conductivity, durability and the membrane performance in electrochemical devices [50]. Water uptake of membranes in the OH^- form cannot be easily determined because of the various equilibrium reactions occurring [52]. The water uptake of the PVA membranes is the highest, because of the huge swelling capacity and hydrophilicity of this polymer that limits its performance in membrane fuel cells [49]. The water uptake of the commercial AAEMs tested in this work agrees with literature [36], and those values are lower than those measured for the membranes prepared in this work because of the large effect of the thick interwoven support providing good mechanical resistance in the case of the FAA and AHA membranes. The water uptake of the AAEMs membranes prepared in this work is close to other zeolite-CS membranes prepared for proton exchange fuel cells [53]. The addition of laminar inorganic fillers provided the lowest water uptake values for CS:PVA membranes, since these fillers likely complete further the free spaces of polymer where the water molecules are lodged, and hence the water can be easily desorbed. Many studies have proven that the casting of polymers with fillers such as SiO_2, or TiO_2, among many other inorganic fillers, reduce the water uptake or lead to a low humidity ascribed mainly to hygroscopic nature of those inorganic fillers [54, 55]. Furthermore, the addition of a hygroscopic oxide results in change in structure of membrane, in which the particles block part of the hydrophilic polymer channels through which protons migrate [56]. In the case

of CS:PVA membranes doped with 4VP and AS4 ionomers, the water uptake is somehow lower than that of the pure PVA and blend CS:PVA membranes because of the hydrophobicity of the ionomers.

IEC indicates the content of ions exchangeable or hydrophilic groups in membrane that contribute to anion or OH^- conductivity and the migration rate of these ions through the membrane. Therefore, IEC is an indirect measure of the membrane conductivity. Generally, a high IEC value is related to a high conductivity although a lower IEC does not always involve a lower conductivity since swelling effects and the mobility of alkaline groups are not taken into account in the IEC measurement [57]. Table 3 also collects the IEC values calculated from equation (3). The IEC values of pure CS and PVA membranes are very low, in agreement with literature [17, 58-60]. This increases upon blending reaching values similar to those of the commercial AAEMs when 5 wt. % of AS4 ionomer or UZAR-S3 stannosilicate are used as fillers. The IEC value increases from 0.253 mmol g^{-1} for CS:PVA membrane to 0.310 and 0.325 mmol g^{-1} for UZAR-S3 and AS4 ionomer added, respectively, because of the decreased crystallinity observed by XRD. In case of adding AM-4 filler, the IEC results to be lower than that one for CS:PVA membrane. The laminar AM-4 structure, which is completely dispersed within the polymer matrix as shown by SEM, may be interacting with the functionalized groups responsible of ion mobility. Regarding the 4VP ionomer, the IEC increases because the anionic ionomer introduces positive groups that facilitate the OH^- transport; however the IEC value of the 4VP/CS:PVA membrane is lower than that of the AS4/CS:PVA membrane. Even though the supplier does not provide the chemical structure of AS4, we speculate that the incorporation of the AS4 filler might be introducing an additional number of OH^- conducting groups. In addition, it is worth noting

that the water uptake value is major for 4VP ionomer and it may contribute to the increased number of OH^- ions in the polymer matrix.

The chemical degradation observed for other AAEM after several days immersion in 1.0 M NaOH at 25 ºC [49] is not observed for the CS:PVA-based MMMs prepared in our laboratory, which lead to the same values of IEC and water uptake (see Table 3) after immersion in 1.0 M NaOH from a few hours to several days. On the other hand, a larger immersion time of membrane in 1.0 M NaOH does not vary the IEC value for the membranes studied in this work. Finally, it is worth taking into account that the chosen ion exchange media, 1.0 M NaOH, in this work has been reported as giving lower conductivity values because, when the OH^- concentration increases, the free degree of transport decreases due to the higher OH^- concentration in polymer [61].

3.2 Ionic conductivity

The typical AC impedance spectra of CS:PVA MMMs are shown in Figure 6 where mostly the Nyquist representation show non-vertical plots. From the Bode plots, the bulk resistance of the membrane, $R_{m,}$ was worked out for all CS:PVA MMMs as in the previous CS-based MMMs [18]. By taking into account the bulk resistance of the membrane, thickness of the membrane and the effective membrane area (1.13 cm^2 in the EIS experiment), the ionic conductivity is obtained according to equation (4). Table 3 also collects the ionic conductivity values of the commercial and CS:PVA MMMs. The ionic conductivity measured is due only to the mobility through the membrane of the OH^- ions present in membrane structure. All membranes, except the UZAR-S3/CS:PVA-membrane, give higher conductivity values than the CS:PVA blend membrane.

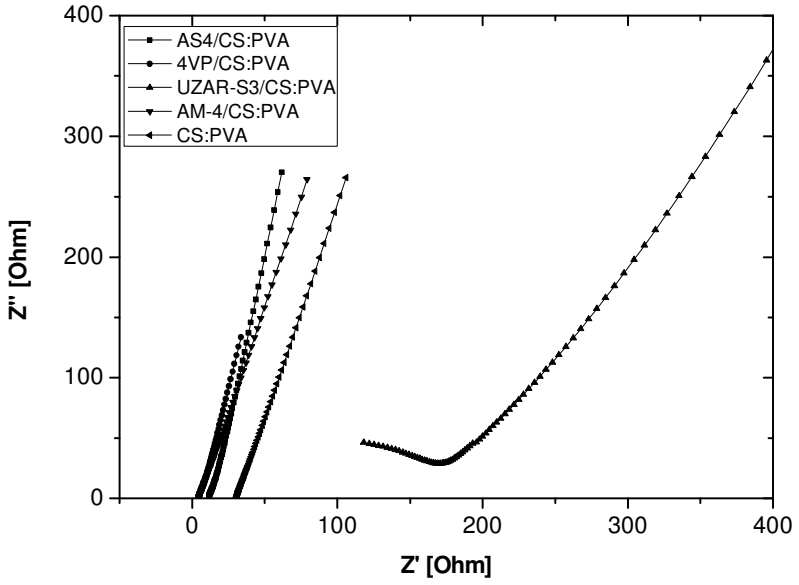

Figure 6. Nyquist plots for the impedance response of the CS:PVA-based membranes at room temperature (100 Hz -1.0 MHz).

The 4VP/CS:PVA MMM show the highest conductivity of 1.15 mS cm^{-1} after activation in 1.0 M NaOH aqueous solution for 24 h and stabilised in ultrapure water for 24 h. The AS4/CS:PVA MMM show a conductivity of 0.325 mS cm^{-1} although their IEC value indicate a larger amount of OH^- exchangeable ions than the 4VP-based membrane that contribute to conductivity. This difference on the conductivity values provided by the organic ionomer could be ascribed to the influence of 4VP on the loss of polymer blend crystallinity, since AS4 ionomer led to a membrane with more crystalline character and only the amorphous part of a membrane is responsible for ion transport across the membrane.

On the other hand, the UZARS-3/CS:PVA MMM give the lowest conductivity, due likely to the dual layer structure of this membrane. Presumably, the top layer of exfoliated UZAR-S3 particles imposes a structural barrier for the OH^- ions mobility across the membrane [57]. In the case of AM-4/CS:PVA, the layered titanosilicate is well

dispersed within the polymer matrix, probably shortening the neighbouring OH^- groups and allowing a higher conductivity value despite the inorganic filler acting as OH^- ions barrier [57].

Even though the ionic conductivity of CS:PVA MMMs was less than one order of magnitude of those of anionic exchange alkaline commercial membranes, with the exception of the 4VP/CS:PVA membrane, the CS:PVA based membranes prepared in this work show up high stability in alkaline conditions, low cost and biodegradability compared to the perfluorinated Nafion membranes. Moreover, the CS:PVA membranes offer a better physical contact with the carbonaceous electrodes because of its low thickness and higher flexibility than commercial membranes such as perfluorinated Nafion or FAA.

3.3 Alcohol permeability

The alcohol permeability is an important parameter in electrochemical devices, since a high alcohol permeation decreases the overall efficiency of the reactor cell. To have an approach of the cross-over that should be avoided upon the electrosynthesis reaction of propargyl alcohol, n-propanol is chosen as model alcohol to measure the permeability across the new AAEM prepared in this work as a function of membrane composition, because of the similarity of structure and lower volatility and toxicity than the propargyl alcohol.

Table 4. Thickness and permeability of n-propanol through the membranes.

Membrane	**Thickness (μm)**	**$P \cdot 10^{-7}$ (cm^2/s)**
CS:PVA	48.5	1.76

4VP/CS:PVA	107	3.63
AS4/CS:PVA	39.3	3.13
AM-4/CS:PVA	102	5.56
UZAR-S3/CS:PVA	82	2.78
FAA (Fumatech)	130	2.34
AHA (Tokuyama)	220	2.50
AMI-7001 [64]	450	22.5
Nafion 117 [65]	N.A.	13.1
Nafion 115 [46]	N.A.	24.2
QSEBS [66]	N.A.	2.34-4.31
PVA-SiO_2 30 wt.% [65]	N.A.	2.00
CS-SiO_2 15 wt.% [15]	N.A.	15.5

N.A. = Not Available in the referenced paper.

Results are collected in Table 4, where the permeability values are in the same order or magnitude or even lower than those values reported for methanol cross-over through other AAEMs in alkaline fuel cells, and lower than most common polyelectrolytes such as Nafion [36, 56-58]. The permeability of n-propanol through the CS:PVA blend membrane is the lowest and, after the incorporation of the layered titanosilicate, and AS4 and 4VP ionomers into the CS:PVA matrix, the n-propanol

permeability increases. This can be related to the loss of crystallinity of the membrane matrix upon hybridization as discussed over Figure 4. Generally, the decrease in crystallinity allows for higher alcohol permeability through the membrane [62] and consequently broadens the matrix channels, thus allowing higher penetration and increase of the ionic conductivity. The results obtained for the AM-4/CS:PVA MMM, where AM-4 particles are homogeneously arranged inside the polymeric matrix with a low degree of crystallinity, according to XRD results (Figure 4), due to probable exfoliation of the layer particles, presents a high n-propanol permeation, offering a poor barrier effect of the titanosilicate filler. On the contrary, the UZAR-S3/CS:PVA MMM show a permeability close to that of the commercial FAA and AHA membranes, widely employed in fuel cell devices [54], and smaller than those of Nafion 117, Nafion 115 and AMI-7001 (see Table 4). This can be attributed to the similar dual layer structure and a better dispersion of the partially exfoliated UZAR-S3 particles but only on the upper membrane layer, thus increasing the tortuosity and decreasing the permeation rate. It is also worth noting that the concentration in compartment B was kept constant for more than 1 h in the case of the AM-4/CS:PVA and UZAR-S3/CS:PVA, FAA and AHA membranes, while it was sharply decreased after 30 min in the other membranes containing the organic ionomers 4VP and AS4.

3.4 Polarisation curves

A plot of cell potential against current density under a set of constant operating conditions, known as a polarisation curve, is the standard electrochemical technique for characterizing the performance of fuel cells [63]. In this study, we use our PEM based electrochemical reactor, PEMER [40], for the examination of the membranes

performance using a steady-state polarisation curve by recording the current intensity as a function of cell potential.

We first investigated cell potentials at open circuit with values of -200, +5, -140, +6, and +5 mV for FAA, AM-4/CS:PVA, UZAR-S3/CS:PVA, 4VP/CS:PVA and AS4/CS:PVA MMMs, respectively. The potential near zero for CS:PVA blend filled with AM-4 and AS4 and 4VP ionomers is attributed to the water swelling and high permeation of n-propanol, respectively, as seen in Tables 3 and 4. Consequently, after 10 min equilibration in the PEMER for feeding the anode compartment with a 0.25 M propargyl alcohol and 1.0 M NaOH solution, and the cathode compartment with humidified air (see experimental section), permeation of NaOH solution and thus water and propargyl alcohol molecules can take place towards the cathode compartment using the latter membranes, leading to near zero potentials at open circuit.

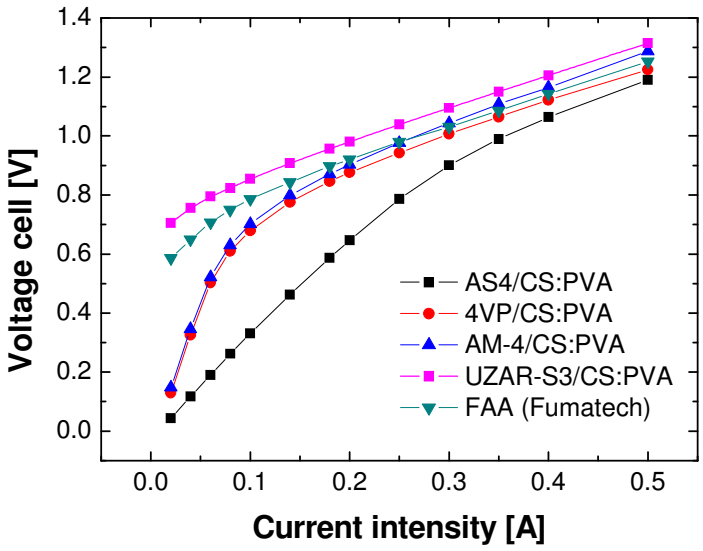

Figure 7. Polarisation curves of FAA membrane and CS:PVA-based membranes in 0.25 M propargyl alcohol in 1.0 M NaOH solution. The current intensity ranges from 0.020 A

to 0.500 A. Each current intensity value is held for 1 min before recording the cell potential.

Figure 7 depicts the polarisation curves in the presence of propargyl alcohol for each of the synthesised membranes and the FAA membrane from Fumatech GmbH, as control membrane. Even though the 4VP/CS:PVA membranes showed the highest ionic conductivity, other IR drops exist that contribute to the enhancement of the electrochemical reactor cell potential. Assuming the same anode and cathode electrode potentials under any certain experimental condition, the difference in the polarisation plot could be ascribed to the IR drop of the membrane and internal IR drops associated with membrane to electrode contact resistances. According to equation (6), cell potential comprises the sum of anode and cathode electrode potentials at open-circuit, anodic and cathodic overpotentials and IR drops.

$$E_{cel} = E_{an} - E_{cat} + \sum IR = E_{I=0} + \left(\eta_{an} - \eta_{cat}\right) + \sum IR \qquad (6)$$

where E denotes electrode potential for the anode and cathode, $E_{I=0}$ is the electrode potential at open circuit, I is the current intensity and R the resistance, and η_{an} and η_{cat} correspond to the anodic and cathodic overpotentials, respectively. It is worth noting that IR is a contribution of potential drops related to the external circuits, the membrane resistance, the resistances of the catholyte and anolyte as well as the contact resistance between membrane and electrodes.

More specifically, differences found in the IR drops of the 4VP/CS:PVA and AS4/CS:PVA membranes were remarkably small at 0.02 A (*circa* 3 mV). This means that the lowest cell potential showed in Figure 7 as a function of current intensity for the AS4/CS:PVA membrane is easily ascribed to a lower contact resistance between the membrane itself and the electrodes (anode and cathode). The above argumentation is

likely associated with a lower membrane thickness and consequently a higher membrane flexibility, which favours an optimum contact with the carbonaceous electrodes providing hence lower cell potentials.

On the other hand, polarisation plots of AM-4/CS:PVA and 4VP/CS:PVA membranes were identical, although the ionic conductivities of both membranes were remarkably different. However, similarities in surface roughness, water uptake and membrane thickness were variables that dominate a similar polarisation response, as shown in Figure 7.

Cell potential increases linearly with current intensity for all membranes. However, we note a high *R* for the CS:PVA MMM filled with 4VP and AM-4 until a current intensity of 0.1 A is reached, whilst a lower *R* drop, similar to that obtained using the FAA membrane, is obtained for the UZAR-S3/CS:PVA MMM. On the other hand, the AS4/CS:PVA MMM shows a moderate *R* until a set current intensity of 0.4 A is reached. The first part of the polarisation curve can be ascribed to the activation of the cathode process associated to the oxygen reduction reaction. The reactivation of the membrane is discarded since the polarisation curves are almost identical after repetitive experiments carried out with different batches of membrane.

After obtaining the polarisation curves, the cathode compartment is moderately wet when using the CS:PVA based membranes with higher permeation. On the contrary, the UZAR-S3/CS:PVA- and the commercial FAA membrane prevent very effectively the pass of solvent to the cathode compartment, keeping the air gas diffusion electrode nearly dried. Furthermore, the performance of UZAR-S3/CS:PVA composite membrane under the polarisation conditions is similar to the commercial FAA membrane with a constant *IR* drop within the current intensity interval studied. If the same IR drops associated with the membrane and electrode contact are considered and the thickness is normalised to the

same value of 130 μm for both membranes, the IR drops obtained for the FAA and UZAR-S3/CS:PVA membranes would be about 3.6 mV and 340 mV, respectively, with a set current intensity of 0.02 A. The difference in potential of circa 336 mV becomes 214 mV when considering the real thickness of the UZAR-S3/CS:PVA membrane (according to data from Table 4). The difference obtained in cell potential is almost constant irrespective of the set current intensity. Hence, this scenario is clearly advantageous for the selection of the FAA membrane. Nonetheless, the cell potential contribution along the electrochemical reactor PEMER is more complex. In this regard, besides the ionic conductivity difference between both membranes, the lower rigidity of the UZAR-S3/CS:PVA membrane compared to the commercial FAA membrane provides a better physical contact with the carbonaceous electrodes, giving rise to a reduced IR contact drop between the membrane and the electrodes. The improvement in cell performance using this membrane may be due to the barrier posed by the UZAR-S3 layers to alcohol permeation.

Regarding the high conductivity 4VP/CS:PVA membrane, clearly, the anionic ionomer acts as binder of the catalyst layer supported on Toray carbonaceous electrode as well as favours OH- conductivity throughout the catalytic layers. Therefore, we believe that the polarisation performance of FAA membrane could not be much better than that of the 4VP/CS:PVA for two main reasons. Firstly, the OH- conductivity of the FAA membrane is similar to that of the 4VP/CS:PVA membrane and, secondly, the attachment of the membrane with the electrode is only achieved by physical contact under some pressure submitted by the bipolar plates and not by hot pressing as commonly performed for the MEA manufacture in fuel cells [67].

The study of the polarisation curves demonstrates the feasibility and viability of alkaline CS:PVA MMMs filled with organic ionomers and inorganic layered

titanosilicates and stannosilicates in a PEM electrochemical reactor (PEMER). A PEMER involves an anode of non-noble metals –nickel nanoparticles- and the air electrode using Pt metal catalyst, allowing a good activity for the reduction of O_2 to OH^- in an alkaline medium. Another advantage is that the manufacturing of CS:PVA as a separator solid electrolyte is a biodegradable, cheap hydrocarbon polymer membrane, as compared with the expensive perfluorosulfonated Nafion membrane.

Preliminary studies on the durability of CS:PVA based membranes were obtained by submitting each membrane to a constant current density of 10 mA cm^{-2} (current intensity of 0.250 A) for 5 h in the PEMER under the experimental conditions described in the Experimental section. Cell potential remained constant at a value between 0.8 and 1.0 V. Nevertheless, it is still necessary to complete the physico-chemical characterization and the durability tests of the CS:PVA- based membranes after their use, which is out of the scope of this work and will be addressed in the near future.

4. Conclusions

The main properties of the membrane influencing the performance of a PEM electrochemical reactor are structural, thermal and chemical stability, controllable water uptake and swelling, ionic conductivity and durability. In this work, MMM were prepared from equimolar CS:PVA blends filled with organic (AS4 and 4VP anionic ionomers) or inorganic (AM-4 and UZAR-S3 layered silicates) fillers. These membranes were characterised by TGA, XPS, XRD, SEM, water uptake, ion exchange capacity (IEC) and EIS. XPS reveals that chemical bonding rather than electrostatic interactions dominate the attachment between the polymer blend and anionic ionomers, which leads to higher thermal stability and a very similar decomposition temperature for all the CS:PVA MMM. All the fillers are homogeneously dispersed in the CS:PVA polymer blend, except

UZAR-S3, which presents a dual layer structure that provides a structural barrier to the mobility of hydroxide ions and alcohol through the membrane, providing lower conductivity and permeability than the AM-4 inorganic filler. The better dispersion of the latter inside the polymer matrix leads to a lower water uptake and bridging over the neighbouring hydroxide conductive groups of AM-4 layers and CS:PVA blend, hence improving the conductivity of the CS:PVA blend, but not reducing the permeability. The AS4 ionomer provides the largest value of IEC but the interaction of the AS4 molecule with the polymer blend seems to promote difficult pathways for the OH^- ion transport through the membrane, and the highest conductivity obtained is that of the 4VP/CS:PVA membrane, 1.15 mS cm^{-1}. The CS:PVA blend membranes have an IEC almost as large as that of 4VP/CS:PVA MMM and higher conductivity than the pure polymers, as well as the lowest propanol permeability due to the higher crystallinity degree. The behaviour of UZAR-S3/CS:PVA MMM in the polarisation curves is similar to that of the commercial FAA membrane, probably because of a closer contact with both the anode and cathode electrodes and consequently a significant reduction in the cell potential, while the FAA membrane is more rigid and stiff.

These results show the promising potential of layered stannosilicate UZAR-S3 and anionic 4VP ionomer to improve the performance of AAEMs in the enhancement of the PEMER efficiency. The findings of this work suggest that CS:PVA based MMM approach is a feasible way of obtaining promising hydroxide exchange membranes for polymer electrolyte membrane applications with tuneable cross-over.

5. Acknowledgements

We gratefully acknowledge the financial support from the Spanish Ministry of Economy and Competitiveness (MINECO) for CTQ2012-31229 project at the University

of Cantabria, and MINECO-FEDER through the CTQ2013-48280-C3-3-R project at the University of Alicante. C. C. C. also thanks the MINECO for the "Ramón y Cajal" program at the University of Cantabria (RYC2011-08550), and L. G. C. for her PhD fellowship BES-2011-045147 and the EEBB-14-09094 mobility grant for the research stay at the University of Cantabria, respectively. Dr. César Rubio, Prof. Carlos Téllez and Prof. Joaquín Coronas from the University of Zaragoza are also warmly thanked for the UZAR-S3 sample.

6. References

[1] A. Saez, V. Garcia-Garcia, J. Solla-Gullon, A. Aldaz, V. Montiel, Electrocatalytic hydrogenation of acetophenone using a Polymer Electrolyte Membrane Electrochemical Reactor, Electrochim. Acta, 91 (2013) 69-74.

[2] V. Montiel, A. Saez, E. Exposito, V. Garcia-Garcia, A. Aldaz, Use of MEA technology in the synthesis of pharmaceutical compounds: The electrosynthesis of N-acetyl-L-cysteine, Electrochem. Commun., 12 (2010) 118-121.

[3] Z. Rong, J.R. Varcoe, Alkaline Anion Exchange Membranes for Fuel Cells: A Patent Review, Recent Pat. Chem. Eng., 4 (2011) 93-115.

[4] G. Merle, M. Wessling, K. Nijmeijer, Anion exchange membranes for alkaline fuel cells: A review, J. Membr. Sci., 377 (2011) 1-35.

[5] M. Carmo, G. Doubek, R.C. Sekol, M. Linardi, A.D. Taylor, Development and electrochemical studies of membrane electrode assemblies for polymer electrolyte alkaline fuel cells using FAA membrane and ionomer, J. Power Sources, 230 (2013) 169-175.

[6] Y.-J. Wang, J. Qiao, R. Baker, J. Zhang, Alkaline polymer electrolyte membranes for fuel cell applications, Chem. Soc. Rev., 42 (2013) 5768-5787.

[7] E. Antolini, E.R. Gonzalez, Alkaline direct alcohol fuel cells, J. Power Sources, 195 (2010) 3431-3450.

[8] J. Ma, Y. Sahai, Chitosan biopolymer for fuel cell applications, Carbohydr. Polym., 92 (2013) 955-975.

[9] M.M. Hasani-Sadrabadi, E. Dashtimoghadam, N. Mokarram, F.S. Majedi, K.I. Jacob, Triple-layer proton exchange membranes based on chitosan biopolymer with reduced methanol crossover for high-performance direct methanol fuel cells application, Polymer, 53 (2012) 2643-2651.

[10] D. Xu, S. Hein, K. Wang, Chitosan membrane in separation applications, Mater. Sci. Technol., 24 (2008) 1076-1087.

[11] Y. Zhu, S. Xia, G. Liu, W. Jin, Preparation of ceramic-supported poly(vinyl alcohol)-chitosan composite membranes and their applications in pervaporation dehydration of organic/water mixtures, J. Membr. Sci., 349 (2010) 341-348.

[12] C. Casado-Coterillo, F. Andres, C. Tellez, J. Coronas, A. Irabien, Synthesis and characterization of ETS-10/chitosan nanocomposite membranes for pervaporation, Sep. Sci. Technol., 49 (2014) 1903-1909.

[13] J.H. Fu, J. Ji, W.Y. Yuan, J.C. Shen, Construction of anti-adhesive and antibacterial multilayer films via layer-by-layer assembly of heparin and chitosan, Biomaterials, 26 (2005) 6684-6692.

[14] R.G. de Paiva, M.A. de Moraes, F.C. de Godoi, M.M. Beppu, Multilayer biopolymer membranes containing copper for antibacterial applications, J. Appl. Polym. Sci., 126 (2012) E17-E24.

[15] H. Wu, W. Hou, J. Wang, L. Xiao, Z. Jiang, Preparation and properties of hybrid direct methanol fuel cell membranes by embedding organophosphorylated titania

submicrospheres into a chitosan polymer matrix, J. Power Sources, 195 (2010) 4104-4113.

[16] J. Wang, Y. Zhang, H. Wu, L. Xiao, Z. Jiang, Fabrication and performances of solid superacid embedded chitosan hybrid membranes for direct methanol fuel cell, J. Power Sources, 195 (2010) 2526-2533.

[17] H. Wu, B. Zheng, X. Zheng, J. Wang, W. Yuan, Z. Jiang, Surface-modified Y zeolite-filled chitosan membrane for direct methanol fuel cell, J. Power Sources, 173 (2007) 842-852.

[18] L. Garcia-Cruz, C. Casado-Coterillo, J. Iniesta, V. Montiel, A. Irabien, Preparation and characterization of novel chitosan-based mixed matrix membranes resistant in alkaline media, J. Appl. Polym. Sci., 132 (2015) 42240-42240.

[19] J. Maiti, N. Kakati, S.H. Lee, S.H. Jee, B. Viswanathan, Y.S. Yoon, Where do poly(vinyl alcohol) based membranes stand in relation to Nafion (R) for direct methanol fuel cell applications?, J. Power Sources, 216 (2012) 48-66.

[20] Y. Xiong, Q.L. Liu, Q.G. Zhang, A.M. Zhu, Synthesis and characterization of cross-linked quaternized poly(vinyl alcohol)/chitosan composite anion exchange membranes for fuel cells, J. Power Sources, 183 (2008) 447-453.

[21] B. Smitha, S. Sridhar, A.A. Khan, Synthesis and characterization of poly(vinyl alcoho)-based membranes for direct methanol fuel cell, J. Appl. Polym. Sci., 95 (2005) 1154-1163.

[22] M.H. Buraidah, A.K. Arof, Characterization of chitosan/PVA blended electrolyte doped with NH_4I, J. Non-Cryst. Solids, 357 (2011) 3261-3266.

[23] Y. Wan, B. Peppley, K.A.M. Creber, V.T. Bui, E. Halliop, Preliminary evaluation of an alkaline chitosan-based membrane fuel cell, J. Power Sources, 162 (2006) 105-113.

[24] X. Feng, X. Wang, W. Xing, B. Yu, L. Song, Y. Hu, Simultaneous reduction and surface functionalization of graphene oxide by chitosan and their synergistic reinforcing effects in PVA Films, Ind. Eng. Chem. Res., 52 (2013) 12906-12914.

[25] J.-M. Yang, S.-A. Wang, Preparation of graphene-based poly(vinyl alcohol)/chitosan nanocomposites membrane for alkaline solid electrolytes membrane, J. Membr. Sci., 477 (2015) 49-57.

[26] Y. Zhang, Z. Cui, C. Liu, W. Xing, J. Zhang, Implantation of Nafion (R) ionomer into polyvinyl alcohol/chitosan composites to form novel proton-conducting membranes for direct methanol fuel cells, J. Power Sources, 194 (2009) 730-736.

[27] K. Matsuoka, Y. Iriyama, T. Abe, M. Matsuoka, Z. Ogumi, Alkaline direct alcohol fuel cells using an anion exchange membrane, J. Power Sources, 150 (2005) 27-31.

[28] Y. Leng, G. Chen, A.J. Mendoza, T.B. Tighe, M.A. Hickner, C.-Y. Wang, Solid-state water electrolysis with an alkaline membrane, J. Am. Chem. Soc., 134 (2012) 9054-9057.

[29] L. Franck-Lacaze, P. Sistat, P. Huguet, Determination of the pK(a) of poly (4-vinylpyridine)-based weak anion exchange membranes for the investigation of the side proton leakage, J. Membr. Sci., 326 (2009) 650-658.

[30] E.H. Yu, U. Krewer, K. Scott, Principles and materials aspects of Direct Alkaline Alcohol Fuel Cells, Energies, 3 (2010) 1499-1528.

[31] E.H. Yu, K. Scott, Development of direct methanol alkaline fuel cells using anion exchange membranes, J. Power Sources, 137 (2004) 248-256.

[32] C. Casado, D. Ambroj, Á. Mayoral, E. Vispe, C. Téllez, J. Coronas, Synthesis, swelling, and exfoliation of microporous lamellar titanosilicate AM-4, Eur. J. Inor. Chem., 2011 (2011) 2247-2253.

[33] J. Pérez-Carvajal, P. Lalueza, C. Casado, C. Téllez, J. Coronas, Layered titanosilicates JDF-L1 and AM-4 for biocide applications, Appl. Clay Sci., 56 (2012) 30-35.

[34] C. Rubio, B. Murillo, C. Casado-Coterillo, A. Mayoral, C. Téllez, J. Coronas, Á. Berenguer-Murcia, D. Cazorla-Amorós, Development of exfoliated layered stannosilicate for hydrogen adsorption, Int. J. Hydrogen Energ., 39 (2014) 13180-13188.

[35] J.M. Yang, H.C. Chiu, Preparation and characterization of polyvinyl alcohol/chitosan blended membrane for alkaline direct methanol fuel cells, J. Membr. Sci., 419 (2012) 65-71.

[36] L. Franck-Lacaze, P. Sistat, P. Huguet, Determination of pKa of poly(4-vinylpyridine)-based weak anion exchange membranes for the investigation of the side proton leakage, J. Membr. Sci., 326 (2009) 650-658.

[37] B. Lin, H. Dong, Y. Li, Z. Si, F. Gu, F. Yan, Alkaline stable C2-substituted imidazolium-based anion exchange membranes, Chem. Mater., 25 (2013) 1858-1867.

[38] S.-H. Yun, S.-H. Shin, J.-Y. Lee, S.-J. Seo, S.-H. Oh, Y.-W. Choi, S.-H. Moon, Effect of pressure on through-plane proton conductivity of polymer electrolyte membranes, J. Membr. Sci., 417 (2012) 210-216.

[39] S.M.R. Niya, M. Hoorfar, Study of proton exchange membrane fuel cells using electrochemical impedance spectroscopy technique - A review, J. Power Sources, 240 (2013) 281-293.

[40] V. Montiel, A. Saez, E. Exposito, V. Garcia-Garcia, A. Aldaz, Use of MEA technology in the synthesis of pharmaceutical compounds: The electrosynthesis of N-acetyl-L-cysteine, Electrochem. Commun., 12 (2010) 118-121.

[41] A. Fernandez-Barquin, C. Casado-Coterillo, M. Palomino, S. Valencia, A. Irabien, LTA/Poly(1-trimethylsilyl-1-propyne) mixed-matrix membranes for high-temperature CO_2/N_2 separation, Chem. Eng. Technol, 38 (2015) 658-666.

[42] V. Nafisi, M.-B. Hagg, Development of dual layer of ZIF-8/PEBAX-2533 mixed matrix membrane for CO_2 capture, J. Membr. Sci., 459 (2014) 244-255.

[43] C. Rubio, B. Murillo, C. Casado-Coterillo, A. Mayoral, C. Tellez, J. Coronas, A. Berenguer-Murcia, D. Cazorla-Amoros, Development of exfoliated layered stannosilicate for hydrogen adsorption, Int. J. Hydrogen Energ., 39 (2014) 13180-13188.

[44] E.M. Abdelrazek, I.S. Elashmawi, S. Labeeb, Chitosan filler effects on the experimental characterization, spectroscopic investigation and thermal studies of PVA/PVP blend films, Physica B, 405 (2010) 2021-2027.

[45] C. Casado, D. Ambroj, A. Mayoral, E. Vispe, C. Tellez, J. Coronas, Synthesis, swelling, and exfoliation of microporous lamellar titanosilicate AM-4, Eur. J. Inorg. Chem., (2011) 2247-2253.

[46] J. Wang, L. Wang, Preparation and properties of organic-inorganic alkaline hybrid membranes for direct methanol fuel cell application, Solid State Ionics, 255 (2014) 96-103.

[47] J. Wang, X. Zheng, H. Wu, B. Zheng, Z. Jiang, X. Hao, B. Wang, Effect of zeolites on chitosan/zeolite hybrid membranes for direct methanol fuel cell, J. Power Sources, 178 (2008) 9-19.

[48] Y. Wu, C. Wu, T. Xu, Y. Fu, Novel anion-exchange organic-inorganic hybrid membranes prepared through sol-gel reaction of multi-alkoxy precursors, J. Membr. Sci., 329 (2009) 236-245.

[49] G. Merle, S.S. Hosseiny, M. Wessling, K. Nijmeijer, New cross-linked PVA based polymer electrolyte membranes for alkaline fuel cells, J. Membr. Sci., 409-410 (2012) 191-199.

[50] J.-H. Jeon, R.K. Cheedarala, C.-D. Kee, I.-K. Oh, Dry-type artificial muscles based on pendent sulfonated chitosan and functionalized graphene oxide for greatly enhanced ionic interactions and mechanical stiffness, Adv. Funct. Mater., 23 (2013) 6007-6018.

[51] C. Casado-Coterillo, M.d.M. López-Guerrero, A. Irabien, Synthesis and characterisation of ETS-10/Acetate-based ionic liquid/chitosan mixed matrix membranes for CO_2/N_2 separation, Membranes, 4 (2014) 287-301.

[52] D. Henkensmeier, H. Cho, M. Brela, A. Michalak, A. Dyck, W. Germer, N.M.H. Duong, J.H. Jang, H.-J. Kim, N.-S. Woo, T.-H. Lim, Anion conducting polymers based on ether linked polybenzimidazole (PBI-OO), Int. J. Hydrogen Energ., 39 (2014) 2842-2853.

[53] H. Wu, B. Zheng, X. Zheng, J. Wang, W. Yuan, Z. Jiang, Surface-modified Y zeolite - filled chitosan membrane for direct methanol fuel cell, J. Power Sources, 173 (2007) 842-852.

[54] C.-C. Yang, Y.J. Li, T.-H. Liou, Preparation of novel poly(vinyl alcohol)/SiO_2 nanocomposite membranes by a sol-gel process and their application on alkaline DMFCs, Desalination, 276 (2011) 366-372.

[55] M. Watanabe, H. Uchida, Y. Seki, M. Emori, P. Stonehart, Self-humidifying polymer electrolyte membranes for fuel cells, J. Electrochem. Soc., 143 (1996) 3847-3852.

[56] W.H.J. Hogarth, J.C.D. da Costa, G.Q. Lu, Solid acid membranes for high temperature (> 140 ºC) proton exchange membrane fuel cells, J. Power Sources, 142 (2005) 223-237.

[57] J. Wang, G. He, X. Wu, X. Yan, Y. Zhang, Y. Wang, L. Du, Crosslinked poly (ether ether ketone) hydroxide exchange membranes with improved conductivity, J. Membr. Sci., 459 (2014) 86-95.

[58] Z. Jiang, X. Zheng, H. Wu, J. Wang, Y. Wang, Proton conducting CS/P(AA-AMPS) membrane with reduced methanol permeability for DMFCs, J. Power Sources, 180 (2008) 143-153.

[59] Z. Jiang, X. Zheng, H. Wu, F. Pan, Proton conducting membranes prepared by incorporation of organophosphorus acids into alcohol barrier polymers for direct methanol fuel cells, J. Power Sources, 185 (2008) 85-94.

[60] E.D. Wang, T.S. Zhao, W.W. Yang, Poly (vinyl alcohol)/3-(trimethylammonium) propyl-functionalized silica hybrid membranes for alkaline direct ethanol fuel cells, Int. J. Hydrogen Energ., 35 (2010) 2183-2189.

[61] J. Zhang, J. Qiao, G. Jiang, L. Liu, Y. Liu, Cross-linked poly(vinyl alcohol)/poly (diallyldimethylammonium chloride) as anion-exchange membrane for fuel cell applications, J. Power Sources, 240 (2013) 359-367.

[62] B.P. Tripathi, V.K. Shahi, Functionalized organic-inorganic nanostructured N-p-carboxy benzyl chitosan-silica-PVA hybrid polyelectrolyte complex as proton exchange membrane for DMFC applications, J. Phys. Chem. B, 112 (2008) 15678-15690.

[63] F. Barbir, PEM Fuel Cells: Theory and Practice, Academic Press, 2013.

[64] R. Vinodh and D. Sangeetha, Comparative study of composite membranes from nano-metal-oxide-incorporated polymer electrolytes for direct methanol alkaline fuel cells. J. Appl. Polym. Sci., 128 (2013) 1930-1938.

[65] B.P. Tripathi, M. Kumar, A. Saxena, V.K. Shahi, Bifunctionalized organic-inorganic charged nanocomposite membrane for pervaporation dehydration of ethanol, J. Coll. Int. Sci., 346 (2010) 54-60.

[66] Q.H. Zeng, Q.L. Liu, I. Broadwell, A.M. Zhu, Y. Xiong, X.P. Tu, Anion exchange membranes on quaternized polystyrene-block-poly(ethylene-ran-butylene)-block-polystyrene for direct methanol alkaline fuel cells, J. Membr. Sci., 349 (2010) 237-243.

[67] A. Satasalo-Aarnio, S. Tuomi, K. Jalkanen, K. Kontturi, T. Kallio, The correlation of electrochemical and fuel cell results for alcohol oxidation in acidic and alkaline media, Electrochem. Acta, 87 (2013) 730-738.

Figures captions

Figure 1. Structure of laminar inorganic and organic fillers added: (a) Poly (4-vinylpyridine) cross-linked, methyl chloride quaternary, and (b) (0 0 1) projection of AM-4 titanosilicate.

Figure 2. Photography's of the CS:PVA based membranes synthesised: (a) pristine CS:PVA blend, (b) 4VP/CS:PVA MMM, (c) AS4/CS:PVA MMM, (d) UZAR/S3/CS:PVA MMM and AM-4/CS:PVA MMM.

Figure 3. SEM photographs of the CS:PVA-based membranes: (A) pristine CS:PVA, (B) AS4/CS:PVA, (C) 4VP/CS:PVA, (D) AM-4/CS:PVA, (E) UZAR-S3/CS:PVA. Figures represent the topographical surface (left column) and cross-sectional (right column) view of the membranes.

Figure 4. X-ray diffractograms of the CS:PVA-based membranes.

Figure 5. Thermal decomposition of the CS:PVA-based membranes under nitrogen atmosphere: (a) Comparison of pure polymer and commercial membranes and (b) comparison of CS:PVA-based membranes.

Figure 6. Nyquist plots for the impedance response of the CS:PVA-based membranes at room temperature (100 Hz -1.0 MHz).

Figure 7. Polarisation curves of FAA membrane and CS:PVA-based membranes in 0.25M propargyl alcohol in 1.0 M NaOH solution. The current intensity ranges from

0.020 A to 0.500 A. Each current intensity value is held for 1 min before recording the cell potential.

Table Captions

Table 1. Deconvolution of the XPS Spectra obtained for the CS:PVA, AS4/CS: PVA, 4VP/CS:PVA, UZAR-S3/CS: PVA, and AM-4/CS:PVA MMM, and the assignments based on the binding energy.

Table 2. Membrane decomposition temperature and weight loss. Data are obtained from TGA curves under nitrogen atmosphere.

Table 3. Bound water content, water uptake, ion exchange capacity and hydroxide ion conductivity of the membranes prepared in this work.

Table 4. Thickness and permeability of n-propanol through the membranes.